

Optimal Momentum Management Controller for the Space Station

J. W. Sunkel*

NASA Johnson Space Center, Houston, Texas 77058

and

L. S. Shieh†

University of Houston, Houston, Texas 77204-4793

This paper presents a new sequential design procedure for determining an optimal control moment gyro momentum management and attitude control system for the Space Station Freedom. First, the space station equations of motion are linearized and uncoupled, and the associated state space equations are defined. Next, a new sequential procedure is used for the development of a linear quadratic regulator with eigenvalue placement in a specified region of the complex plane. The regional pole assignment method is used since it is best suited for tradeoffs between eigenvalue locations and robustness with respect to parameter variations, sensor failures, implementation accuracies, and gain reduction. The matrix sign function is used for solving the Riccati equations, which appear in the design procedure. Simulation results are given which show that the resultant design provides desired system performance.

Introduction

PHYSICAL realizations of engineering systems result, in general, in large-scale models. In most cases, it is impractical to consider the analysis and design of the large-scale system model itself. This is the case with the model representing the space station dynamics. Therefore, the necessity arises for decomposing the original system into decoupled subsystems, each with their own distinct characteristics, thus facilitating the application of the well-known analysis and design methods in control theory to subsystems of small order.

Two approaches to decomposing the space station model into decoupled subsystems are possible. The first of these is an algebraic method¹ based on the matrix sign function² for separating the dominant from the nondominant modes of a large-scale multivariable system. Fast and stable algorithms have recently been developed for the computation of the matrix sign function.³

The second approach derives from the dynamics of the "phase 1" space station shown in Fig. 1. Small products of inertia in the equations of motion permit pitch motion to be uncoupled from roll/yaw motion (see Refs. 4 and 5). This paper will follow the second approach and, consequently, pitch control and roll/yaw control will be treated separately.

The space station shown in Fig. 1 will employ control moment gyros (CMGs) as actuators during normal flight mode operation. Since the CMGs are momentum exchange devices, external control torques must be used to desaturate the CMGs, i.e., bring the momentum back to a nominal value. An approach to CMG momentum management is a "continuous" approach⁶ that integrates the momentum management and attitude control design. A scheme, based on this continuous

approach, has been presented by Wie et al.⁶ for the synthesis of a controller for the space station momentum management and attitude control. In the development of the controller, Wie et al.⁶ have accommodated for aerodynamic disturbance rejection via the use of a cyclic disturbance rejection filter. However, the determination of the feedback gains using the LQR technique is quite arbitrary since it involves trial and error in assigning weighting matrices and also does not always result in desirable closed-loop poles.

In this paper, a systematic approach is developed to synthesize an optimal multivariable controller for the space station momentum management and attitude control. The approach combines the regional pole assignment method and optimal control techniques for determining the optimal feedback gains. The disturbance rejection filter will be accommodated in the proposed design.

The optimal linear quadratic (LQ) design method has several good properties. For instance, the closed-loop system is stable and has good robustness properties provided the weighting matrices satisfy certain positivity conditions.⁷ The transient behavior of the closed-loop system is, however, difficult to determine since there is a complex relation between the weighting matrices and the closed-loop poles. This implies that the weighting matrices have to be determined through trial and error. Pole placement methods have the advantage that the closed-loop poles can be specified. The drawback is the nonuniqueness of choice of feedback for multivariable systems. Furthermore, it is too restrictive to place the poles in predetermined locations⁸ since, for nonlinear systems, the exact location of the closed-loop poles might be difficult to attain for each operational condition. However, the regional pole assignment method is suited for tradeoffs between eigenvalue locations, actuator signal magnitudes, and requirements of robustness against large parameter variations, etc.⁸ It is well known⁸ that if the poles of a system lie within the sector region (hatched) in Fig. 2, then the system responses converge at appropriate speed, and any existing vibrating modes are well damped.

The problem of designing feedback gains to optimally place all the poles of a closed-loop system within a specified region was first studied by Anderson and Moore,⁷ who used a shifted system matrix to obtain an optimal closed-loop system with its eigenvalues lying in the open, left half side of a vertical line on

Received Feb. 2, 1989; revision received May 17, 1989; presented as Paper 89-3473 at the AIAA Guidance, Navigation, and Control Conference, Boston, MA, Aug. 14-16, 1989. Copyright © 1989 by the American Institute of Aeronautics and Astronautics, Inc. No copyright is asserted in the United States under Title 17, U.S. Code. The U.S. Government has a royalty-free license to exercise all rights under the copyright claimed herein for Governmental purposes. All other rights are reserved by the copyright owner.

*Aerospace Engineer, Avionics Systems Division.

†Professor, Department of Electrical Engineering.

the negative real axis. Shieh et al.^{9,10} extended this idea to optimally place the poles within a vertical strip as well as a horizontal strip in the left half plane. Kawasaki and Shimemura¹¹ proposed an iterative procedure to place the poles inside a hyperbola in the left half plane, which is actually an approximation of the sector region shown in Fig. 2. In Ref. 12, a state-space design method has been developed to place the eigenvalues of a general continuous time system within the hatched region of Fig. 2.

Mathematical Models for Momentum Management of the Space Station

The space station in circular orbit is expected to maintain local vertical and local horizontal (LVLH) orientation during normal mode operation. The nonlinear equations of motion in terms of components along the body-fixed control axes can be written as⁶

Space station dynamics ($I_{ij} = I_{ji}$ for $i \neq j$):

$$\begin{bmatrix} I_{11} & I_{12} & I_{13} \\ I_{21} & I_{22} & I_{23} \\ I_{31} & I_{32} & I_{33} \end{bmatrix} \begin{bmatrix} \dot{\omega}_1 \\ \dot{\omega}_2 \\ \dot{\omega}_3 \end{bmatrix} = - \begin{bmatrix} 0 & -\omega_3 & \omega_2 \\ \omega_3 & 0 & -\omega_1 \\ -\omega_2 & \omega_1 & 0 \end{bmatrix} \begin{bmatrix} \omega_1 \\ \omega_2 \\ \omega_3 \end{bmatrix} + 3n^2 \begin{bmatrix} 0 & -c_3 & c_2 \\ c_3 & 0 & -c_1 \\ -c_2 & c_1 & 0 \end{bmatrix} \begin{bmatrix} \omega_1 \\ \omega_2 \\ \omega_3 \end{bmatrix} + \begin{bmatrix} I_{11} & I_{12} & I_{13} \\ I_{21} & I_{22} & I_{23} \\ I_{31} & I_{32} & I_{33} \end{bmatrix} \begin{bmatrix} c_1 \\ c_2 \\ c_3 \end{bmatrix} + \begin{bmatrix} -u_1 + w_1 \\ -u_2 + w_2 \\ -u_3 + w_3 \end{bmatrix} \quad (1)$$

where

$$c_1 \triangleq -\sin\theta_2 \cos\theta_3 \quad (2a)$$

$$c_2 \triangleq \cos\theta_1 \sin\theta_2 \sin\theta_3 + \sin\theta_1 \cos\theta_2 \quad (2b)$$

$$c_3 \triangleq -\sin\theta_1 \sin\theta_2 \sin\theta_3 + \cos\theta_1 \cos\theta_2 \quad (2c)$$

Attitude kinematics (2-3-1 body-axis sequence):

$$\begin{bmatrix} \dot{\theta}_1 \\ \dot{\theta}_2 \\ \dot{\theta}_3 \end{bmatrix} = \frac{1}{\cos\theta_3} \begin{bmatrix} \cos\theta_3 & -\cos\theta_1 \sin\theta_3 & \sin\theta_1 \sin\theta_3 \\ 0 & \cos\theta_1 & -\sin\theta_1 \\ 0 & \sin\theta_1 \cos\theta_3 & \cos\theta_1 \cos\theta_3 \end{bmatrix} \begin{bmatrix} \omega_1 \\ \omega_2 \\ \omega_3 \end{bmatrix} + \begin{bmatrix} 0 \\ n \\ 0 \end{bmatrix} \quad (3)$$

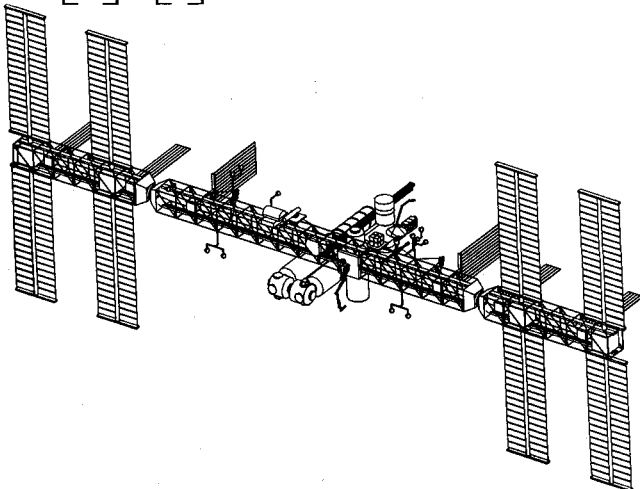


Fig. 1 Phase 1 Space Station Freedom.

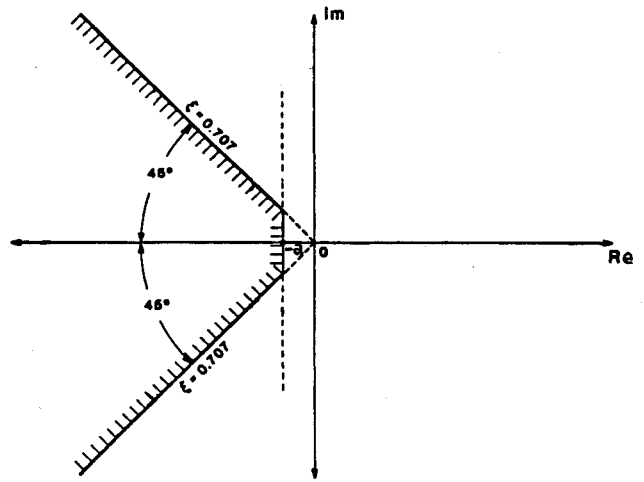


Fig. 2 Pole assignment sector.

CMG momentum:

$$\begin{bmatrix} h_1 \\ h_2 \\ h_3 \end{bmatrix} + \begin{bmatrix} 0 & -\omega_3 & \omega_2 \\ \omega_3 & 0 & -\omega_1 \\ -\omega_2 & \omega_1 & 0 \end{bmatrix} \begin{bmatrix} h_1 \\ h_2 \\ h_3 \end{bmatrix} = \begin{bmatrix} u_1 \\ u_2 \\ u_3 \end{bmatrix} \quad (4)$$

where (1,2,3) are the roll, pitch, and yaw control axes whose origin is fixed at the mass center, with roll axis in the flight direction, the pitch perpendicular to the orbit plane, and the yaw toward the Earth; $(\theta_1, \theta_2, \theta_3)$ are the roll, pitch, and yaw Euler angles of the central (body) axes with respect to LVLH axes, which rotate with the orbital angular velocity, n ; $(\omega_1, \omega_2, \omega_3)$ are the body-axis components of the absolute angular velocity of the station; (I_{11}, I_{22}, I_{33}) are the moments of inertia; $I_{ij} = I_{ji}$ ($i \neq j$) are the products of inertia; (h_1, h_2, h_3) are the body-axis components of the CMG momentum; (u_1, u_2, u_3) are the body-axis components of the control torque caused by the CMG momentum change; (w_1, w_2, w_3) are the body-axis components of the external disturbance torque; and n is the orbital rate of 0.0011 rad/s.

For small attitude deviations from LVLH orientation with an assumption that $n \gg |\Delta\omega_i|$, $i = 1, 2, 3$ where $\Delta\omega = [\omega_1, \omega_2 + n, \omega_3]^T$, the linearized equations of motion can be written as

Space station dynamics ($I_{ij} = I_{ji}$ for $i \neq j$):

$$\begin{bmatrix} I_{11} & I_{12} & I_{13} \\ I_{21} & I_{22} & I_{23} \\ I_{31} & I_{32} & I_{33} \end{bmatrix} \begin{bmatrix} \dot{\omega}_1 \\ \dot{\omega}_2 \\ \dot{\omega}_3 \end{bmatrix} = n \begin{bmatrix} I_{31} & 2I_{32} & I_{33} - I_{22} \\ -I_{32} & 0 & I_{12} \\ I_{22} - I_{11} & -2I_{12} & -I_{13} \end{bmatrix} \begin{bmatrix} \omega_1 \\ \omega_2 \\ \omega_3 \end{bmatrix} + 3n^2 \begin{bmatrix} I_{33} - I_{22} & I_{21} & 0 \\ I_{12} & I_{33} - I_{11} & 0 \\ -I_{13} & -I_{23} & 0 \end{bmatrix} \begin{bmatrix} \theta_1 \\ \theta_2 \\ \theta_3 \end{bmatrix} + n^2 \begin{bmatrix} -2I_{23} \\ 3I_{13} \\ -I_{12} \end{bmatrix} + \begin{bmatrix} -u_1 + w_1 \\ -u_2 + w_2 \\ -u_3 + w_3 \end{bmatrix} \quad (5)$$

Attitude kinematics:

$$\dot{\theta}_1 - n\theta_3 = \omega_1 \quad (6a)$$

$$\dot{\theta}_2 - n = \omega_2 \quad (6b)$$

$$\dot{\theta}_3 + n\theta_1 = \omega_3 \quad (6c)$$

CMG momentum:

$$\dot{h}_1 - nh_3 = u_1 \quad (7a)$$

$$\dot{h}_2 = u_2 \quad (7b)$$

$$\dot{h}_3 + nh_1 = u_3 \quad (7c)$$

Equations (5-7) can be put together and written in the following state-space form:

$$\begin{bmatrix} \dot{\omega} \\ \dot{\theta} \\ \dot{h} \end{bmatrix} = \begin{bmatrix} A_{11} & A_{12} & 0 \\ A_{21} & A_{22} & 0 \\ 0 & 0 & A_{13} \end{bmatrix} \begin{bmatrix} \omega \\ \theta \\ h \end{bmatrix} + \begin{bmatrix} -B \\ 0 \\ Id_3 \end{bmatrix} u + \begin{bmatrix} B \\ 0 \\ 0 \end{bmatrix} w + \begin{bmatrix} d_3 \\ d_2 \\ 0 \end{bmatrix} \quad (8)$$

where ω , θ , h , u , and w are column vectors consisting of ω_i , θ_i , h_i , u_i , and w_i , $i = 1, 2, 3$, respectively. Also,

$$A_{11} = n\hat{f}^{-1} \begin{bmatrix} I_{31} & 2I_{32} & I_{33} - I_{22} \\ -I_{32} & 0 & I_{12} \\ I_{22} - I_{11} & -2I_{12} & -I_{13} \end{bmatrix} \quad (9a)$$

$$A_{12} = 3n^2\hat{f}^{-1} \begin{bmatrix} I_{33} - I_{22} & I_{21} & 0 \\ I_{12} & I_{33} - I_{11} & 0 \\ -I_{13} & -I_{23} & 0 \end{bmatrix} \quad (9b)$$

$$A_{21} = Id_3, \quad A_{22} = A_{13} = \begin{bmatrix} 0 & 0 & n \\ 0 & 0 & 0 \\ -n & 0 & 0 \end{bmatrix} \quad (9c)$$

$$d_3 = n^2\hat{f}^{-1}[-2I_{23}, 3I_{13}, -I_{12}]^T, \quad d_2 = [0, n, 0]^T$$

The cyclic component at orbital rate is due to the diurnal bulge effect, whereas the cyclic torque at twice the orbital rate is caused by the rotating solar panels. The state-space representation in Eq. (8) is the most general form of the three-axis coupled linear equations and will be the basis of our controller design.

For the minimization of the steady-state oscillation of pitch, roll/yaw attitude and CMG momentum, Wie et al.⁶ have proposed appropriate cyclic disturbance filters. These are

$$\ddot{\alpha}_1 + n^2\alpha_1 = h_1, \quad \ddot{\beta}_1 + (2n)^2\beta_1 = h_1 \quad (11a)$$

$$\ddot{\alpha}_i + n^2\alpha_i = \theta_i, \quad \ddot{\beta}_i + (2n)^2\beta_i = \theta_i, \quad i = 2, 3 \quad (11b)$$

The preceding equations can be also written in the following state-space form:

$$\begin{bmatrix} \dot{\alpha} \\ \dot{\alpha} \\ \dot{\beta} \\ \dot{\beta} \end{bmatrix} = \begin{bmatrix} 0 & Id_3 & 0 & 0 \\ -n^2Id_3 & 0 & 0 & 0 \\ 0 & 0 & 0 & Id_3 \\ 0 & 0 & -(2n)^2Id_3 & 0 \end{bmatrix} \begin{bmatrix} \alpha \\ \alpha \\ \beta \\ \beta \end{bmatrix} + \begin{bmatrix} 0 \\ A_h \\ 0 \\ A_h \end{bmatrix} h + \begin{bmatrix} 0 \\ A_\theta \\ 0 \\ A_\theta \end{bmatrix} \theta \quad (12)$$

where α , $\dot{\alpha}$, and $\ddot{\alpha}$ are column vectors consisting of the elements α_i , $\dot{\alpha}_i$, and $\ddot{\alpha}_i$, $i = 1, 2, 3$, respectively. The corresponding vectors in β are also similar. The $A_h = [e_1, 0, 0]$ and $A_\theta = [0, e_2, e_3]$ where $e_1 = [1, 0, 0]^T$, $e_2 = [0, 1, 0]^T$, and $e_3 = [0, 0, 1]^T$. Equation (12) can be joined with the model in Eq. (8) to give us the space station model with cyclic disturbance rejection.

To avoid CMG momentum buildup, we also introduce an integral of the CMG momentum vector h , i.e.,

$$\dot{\hat{h}} = \int h dt \quad \text{or} \quad \dot{\hat{h}} = h \quad (13)$$

Combining Eqs. (12) and (13) with Eq. (8), we obtain the final state-space representation to be used for the control design as

$$\begin{bmatrix} \dot{\omega} \\ \dot{\theta} \\ \dot{h} \\ \dot{\hat{h}} \\ \dot{\alpha} \\ \dot{\alpha} \\ \dot{\beta} \\ \dot{\beta} \end{bmatrix} = \begin{bmatrix} A_{11} & A_{12} & 0 & 0 & 0 & 0 & 0 & 0 \\ A_{21} & A_{22} & 0 & 0 & 0 & 0 & 0 & 0 \\ 0 & 0 & A_{13} & 0 & 0 & 0 & 0 & 0 \\ 0 & 0 & Id_3 & 0 & 0 & 0 & 0 & 0 \\ 0 & 0 & 0 & 0 & 0 & Id_3 & 0 & 0 \\ 0 & A_\theta & A_h & 0 & -n^2Id_3 & 0 & 0 & 0 \\ 0 & 0 & 0 & 0 & 0 & 0 & Id_3 & 0 \\ 0 & A_\theta & A_h & 0 & 0 & 0 & 0 & -(2n)^2Id_3 \end{bmatrix} \begin{bmatrix} \omega \\ \theta \\ h \\ \hat{h} \\ \alpha \\ \alpha \\ \beta \\ \beta \end{bmatrix} + \begin{bmatrix} -B \\ 0 \\ Id_3 \\ 0 \\ 0 \\ 0 \\ 0 \\ 0 \end{bmatrix} u + \begin{bmatrix} B \\ 0 \\ 0 \\ 0 \\ 0 \\ 0 \\ 0 \\ 0 \end{bmatrix} w + \begin{bmatrix} d_3 \\ d_2 \\ 0 \\ 0 \\ 0 \\ 0 \\ 0 \\ 0 \end{bmatrix} \quad (14)$$

and

$$B = \hat{f}^{-1} \quad (9d)$$

The \hat{f} represents the inertia matrix with elements I_{ij} and Id_3 representing a 3×3 identity matrix. The external disturbances (aerodynamic disturbances) w_i are modeled as bias plus cyclic terms in the body-fixed control axes:

$$w_i(t) = \text{bias} + A_n \sin(nt + \phi_n) + A_{2n} \sin(2nt + \phi_{2n}) \quad (10)$$

In the following section, we will introduce optimal regional pole assignment for continuous time systems in a general state-space representation.

Optimal Quadratic Regulators with Pole Placement

Consider the linear controllable continuous time system described by [similar to Eq. (14) without considering w]

$$\dot{x}(t) = Ax(t) + Bu(t); \quad x(0) \quad (15)$$

where $\dot{x}(t)$ and $u(t)$ are the $n \times 1$ state vector and the $m \times 1$ input vector, respectively, and A and B are constant matrices

of appropriate dimensions. Let the quadratic cost function for the system in Eq. (15) be

$$J = \int_0^\infty [x^T(t)Qx(t) + u^T(t)Ru(t)] dt \quad (16)$$

where the weighting matrices Q and R are $n \times n$ nonnegative definite and $m \times m$ positive definite symmetric matrices, respectively. The feedback control law that minimizes the performance index in Eq. (16) is given by Ref. 7:

$$u(t) = -Kx(t) + \hat{r}(t) = -R^{-1}B^TPx(t) + \hat{r}(t) \quad (17)$$

where K is the feedback gain, $\hat{r}(t)$ is a reference input, and P , a $n \times n$ nonnegative definite symmetric matrix, is the solution of the Riccati equation

$$PBR^{-1}B^TP - PA - A^TP - Q = 0_n \quad (18)$$

with (Q, A) detectable. The superscript T and the matrix 0_n denote the transpose and the $n \times n$ null matrix, respectively. Thus the resulting closed-loop system becomes

$$\dot{x}(t) = (A - BK)x(t) + B\hat{r}(t) \quad (19)$$

The eigenvalues of $A - BK$, denoted by $\lambda(A - BK)$, lie in the open, left-half plane of the complex s plane. Our objective is to determine Q , R , and K so that the closed-loop system in Eq. (19) has its eigenvalues on or within the hatched region of Fig. 2. The important results along with the design procedure to achieve the desired design are presented in the following.

Lemma 1^{7,9}: Let (A, B) be the pair of the given open-loop system in Eq. (15). Also, let $\alpha \geq 0$ represent the prescribed degree of relative stability. Then, the eigenvalues of the closed-loop system $A - BR^{-1}B^TP$ lie to the left of the $-\alpha$ vertical line with the matrix P being the solution of the Riccati equation

$$PBR^{-1}B^TP - P(A + \alpha Id_n) - (A + \alpha Id_n)^TP = 0_n \quad (20)$$

where the matrix Id_n is an $n \times n$ identity matrix.

Theorem 1¹²: Let the given stable system matrix $A \in \mathbb{R}^{n \times n}$ have eigenvalues $\hat{\lambda}_i^-$ ($i = 1, \dots, n^-$) lying in the open sector in Fig. 2 with the sector angle ± 45 deg from the negative real axis and the eigenvalues $\hat{\lambda}_i^+$ ($i = 1, \dots, n^+$) outside that sector with $n = n^- + n^+$. Now, consider the two Riccati equations

$$\hat{Q}BR^{-1}B^T\hat{Q} - \hat{Q}(-A^2) - (-A^2)^T\hat{Q} = 0_n \quad (21a)$$

$$PBR^{-1}B^TP - PA - A^TP - \hat{Q} = 0_n \quad (21b)$$

Then, the closed-loop system

$$A_c = A - rBK = A - rBR^{-1}B^TP \quad (22)$$

will enclose the invariant eigenvalues $\hat{\lambda}_i^-$ ($i = 1, \dots, n^-$) and at least one additional pair of complex conjugate eigenvalues lying in the open sector in Fig. 2 for the constant gain r in Eq. (22) satisfying

$$r \geq \max \left\{ \frac{1}{2}, \frac{b + \sqrt{b^2 + ac}}{a} \right\} \quad (23)$$

where $a = \text{tr}[(BR^{-1}B^TP)^2]$, $b = \text{tr}[BR^{-1}B^TPA]$, and $c = (1/2) \times \text{tr}[BR^{-1}B^T\hat{Q}]$.

Remark 1: The steady-state solutions of the Riccati equations in Eqs. (20) and (21) can be found using the matrix sign function techniques,^{13,14} and a brief review of this is given in the Appendix.

Design Procedure

The steps to optimally place all the closed-loop eigenvalues in the hatched region of Fig. 2 are described as follows.

Table 1 Space station parameters

Inertia, slug-ft ²		Aerodynamic torque, ft-lb	
I_{11}	50.28E6	W_1	$1 + \sin(nt) + 0.5 \sin(2nt)$
I_{22}	10.80E6	W_2	$4 + 2 \sin(nt) + 0.5 \sin(2nt)$
I_{33}	58.57E6	W_3	$1 + \sin(nt) + 0.5 \sin(2nt)$
I_{12}	-0.39E6	—	—
I_{13}	0.16E6	—	—
I_{23}	0.16E6	—	—

Step 1

Let the given continuous time system be as in Eq. (15). Specify α so that the $-\alpha$ vertical line on the negative real axis would represent the line beyond which the eigenvalues have to be placed in the sector of Fig. 2. Also, assign $A_0 = A$ and the positive definite matrix R . Set $i = 1$. If the system is unstable, then solve Eq. (20) to obtain the closed-loop system $A_1 = A - r_0BR^{-1}B^TP_0 = A - r_0BK_0$, with $r_0 = 1$; else (stable system) go to step 2 with $A_1 = A$, $P_0 = 0_n$, and $r_0 = 0$.

Step 2

Solve Eq. (21a) for \hat{Q}_i with $A := A_i$. Check if $(1/2) \times \text{tr}[BR^{-1}B^T\hat{Q}_i]$ is zero. If it is equal to zero, go to step 4 with $j = i$; else, continue and go to step 3. Note that when $(1/2) \times \text{tr}[BR^{-1}B^T\hat{Q}_i] = 0$, all eigenvalues of the matrix A_i lie on or within the open sector of Fig. 2.

Step 3

Solve Eq. (21b) for P_i with $A := A_i$ and $\hat{Q} := \hat{Q}_i$. Then, the constant gain r_i can be evaluated using Eq. (23). The closed-loop system matrix is

$$A_{i+1} = A_i - r_iBR^{-1}B^TP_i = A_i - r_iBK_i \quad (24a)$$

Set $i := i + 1$ and go to step 2.

Step 4

Check if $\text{tr}[(A_j + \alpha Id_n)]^+$ (sum of the eigenvalues to the right of the vertical line at $-\alpha$) is zero. If it is equal to zero, go to step 5 with $P_{j+1} = 0_n$ and $r_{j+1} = 0$; else, solve Eq. (20) for P_{j+1} with $A := A_j$ and obtain the closed-loop system $A_j - r_{j+1}BR^{-1}B^TP_{j+1} = A_j - r_{j+1}BK_{j+1}$, with $r_{j+1} = 1$ and $K_{j+1} = R^{-1}B^TP_{j+1}$.

Step 5

The designed closed-loop system is

$$A_0 - BR^{-1}B^T \sum_{k=0}^{j+1} r_k P_k \quad (24b)$$

and its eigenvalues lie in the hatched region of Fig. 2. Note that the preceding system matrix in Eq. (24b) is equal to the system matrix in Eq. (19), $A - BR^{-1}B^T\hat{P}$, where \hat{P} is the solution of the Riccati equation in Eq. (18) with

$$Q = 2\alpha(P_0 + P_{j+1}) + \sum_{i=1}^j (\hat{Q}_i + \Delta r_i P_i BR^{-1}B^TP_i) r_i \quad (25)$$

In the preceding equation, $\Delta r_i = r_i - 1$ and the matrix R is as originally assigned. Also, the optimal continuous time regulator can be given as

$$u(t) = - \left(\sum_{i=0}^{j+1} r_i K_i \right) x(t) + \hat{r}(t) = -Kx(t) + \hat{r}(t) \quad (26)$$

where $\hat{r}(t)$ is any reference input and K is the desired state feedback gain.

Pitch Control Without Disturbance Rejection Filter

The pitch axis controller for the system in Eq. (14) consists of a single input u_2 and four states: θ_2 , ω_2 , h_2 , \dot{h}_2 . The pitch control law is then given by

$$u_2 = -K_{A_2}\theta_2 - K_{R_2}\omega_2 - K_{H_2}h_2 - K_{I_2} \int h_2 \quad (27a)$$

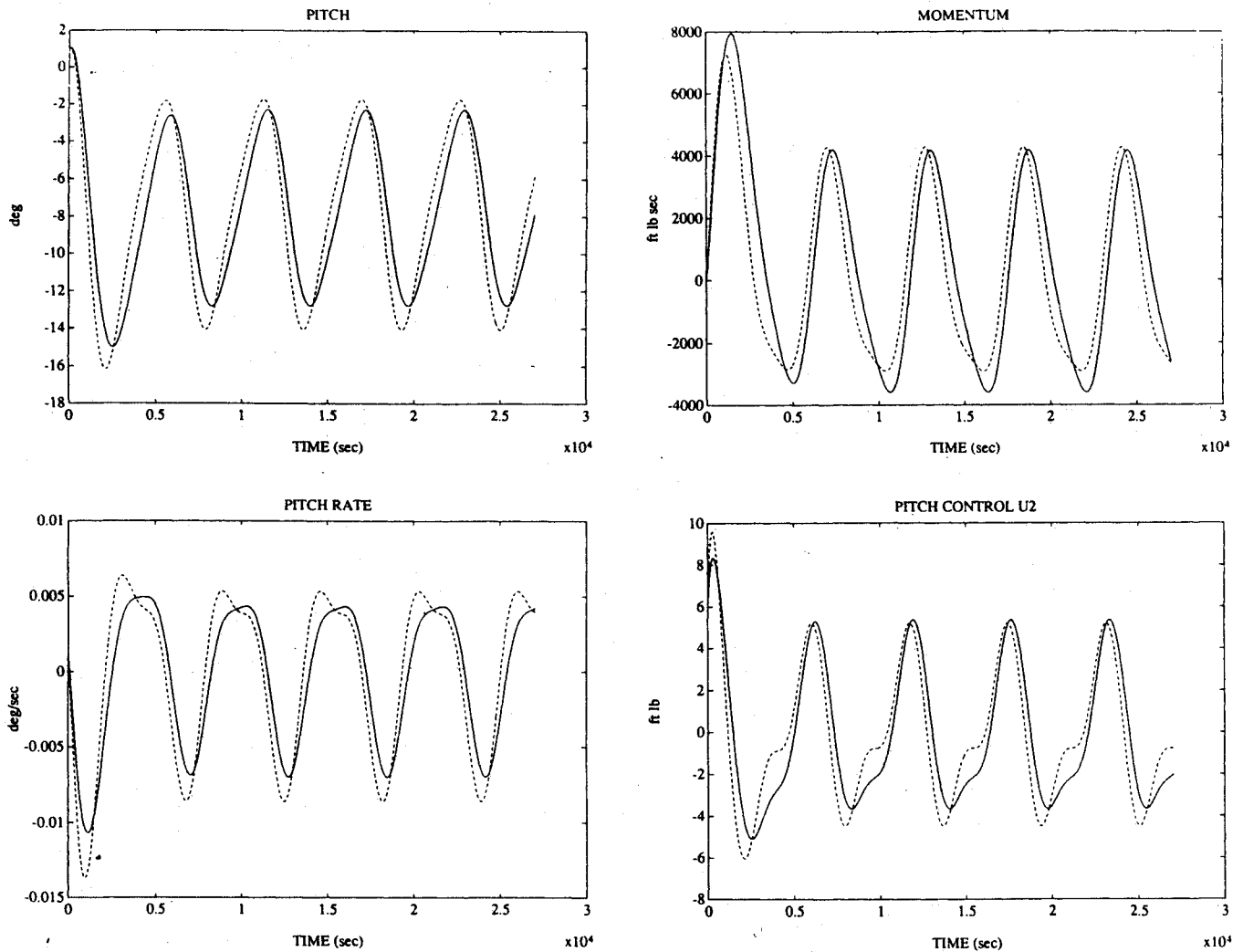


Fig. 3 Pitch axis response without disturbance rejection filter.

Inertial properties of the phase 1 space station are shown in Table 1.

The uncontrolled phase 1 space station is unstable in pitch with poles at $s = \pm 1.52n$ and a double pole at the origin (i.e., $s = 0, 0$). To relocate the unstable double pole at the origin (i.e., $s = 0, 0$) to the stable double pole at $-1.0n$ (i.e., $s = -1.0n, -1.0n$), which has a damping constant equal to $1.0n$, we set the degree of relative stability α in Lemma 1 as $\alpha = 0.5n$ and go to step 1 of the "design procedure" to solve for $A_1 = A - r_0 B R^{-1} B^T P_0$ where $R = Id_n$ and $r_0 = 1.0$. The resulting eigenvalues of matrix A_1 are located at

$$-1.0n, \quad -1.0n, \quad -1.52n, \quad -2.52n$$

From step 2, we solve for \hat{Q}_1 and compute $(1/2)\text{tr}[B R^{-1} B^T \hat{Q}_1]$, which we find equal to zero. Thus, the eigenvalues of the matrix A_1 lie within the open sector of Fig. 2. The corresponding pitch axis control gains are given as follows:

$$K_p \triangleq [K_{A_2} \quad K_{R_2} \quad K_{H_2} \quad K_{I_2}]$$

$$= [-2.2022E2 \quad -1.3193E5 \quad -5.5772E-3 \quad -2.0074E-6]$$

(27b)

The closed-loop response of the system to the aerodynamic disturbance torque listed in Table 1 is shown in Fig. 3. Initial conditions are $\theta_2(0) = 1$ deg, $\omega_2(0) = 0.001$ deg/s, and $h_2(0) = 0$ ft-lb-s. The disturbance torque causes the periodic responses of both pitch attitude and CMG momentum. The pitch atti-

tude oscillates about a -7.5 -deg torque equilibrium attitude (TEA).

Simulation results from Ref. 6 using the LQR approach are included in Fig. 3 for comparison.

Pitch Control with Disturbance Rejection Filter

Depending on the situation, either pitch attitude or CMG momentum oscillation, caused by the aerodynamic disturbance torque, may be undesirable. In that event, a cyclic disturbance rejection filter can be employed as discussed in Ref. 6.

The rejection filter equations for pitch attitude for the system in Eq. (14) are shown in Eq. (11b). The initial conditions for α_2 , β_2 , $\dot{\alpha}_2$, and $\dot{\beta}_2$ were arbitrarily set to zero in this study.

We now repeat the pitch control synthesis of the previous section, augmenting the pitch axis equation with the preceding filter equations. The pitch control law is then given by

$$u_2 = -K_{A_2}\theta_2 - K_{R_2}\omega_2 - K_{H_2}h_2 - K_{I_2} \int h_2 - K_{\alpha_2}\alpha_2 - K_{\dot{\alpha}_2}\dot{\alpha}_2$$

$$- K_{\beta_2}\beta_2 - K_{\dot{\beta}_2}\dot{\beta}_2 \quad (28)$$

The system poles are located at $s = 0, 0, \pm 1.52n, \pm 1.0nj$, and $\pm 2.0nj$. To keep the same degree of relative stability as for the pitch control without the disturbance rejection filter, we use the same α (i.e., $\alpha = 0.5n$) in the design procedure to compute the matrix A_1 with eigenvalues located at

$$-1.0n, \quad -1.0n, \quad -1.52n, \quad -2.52n$$

$$(-1.0 \pm 1.0j)n, \quad (-1.0 \pm 2.0j)n$$

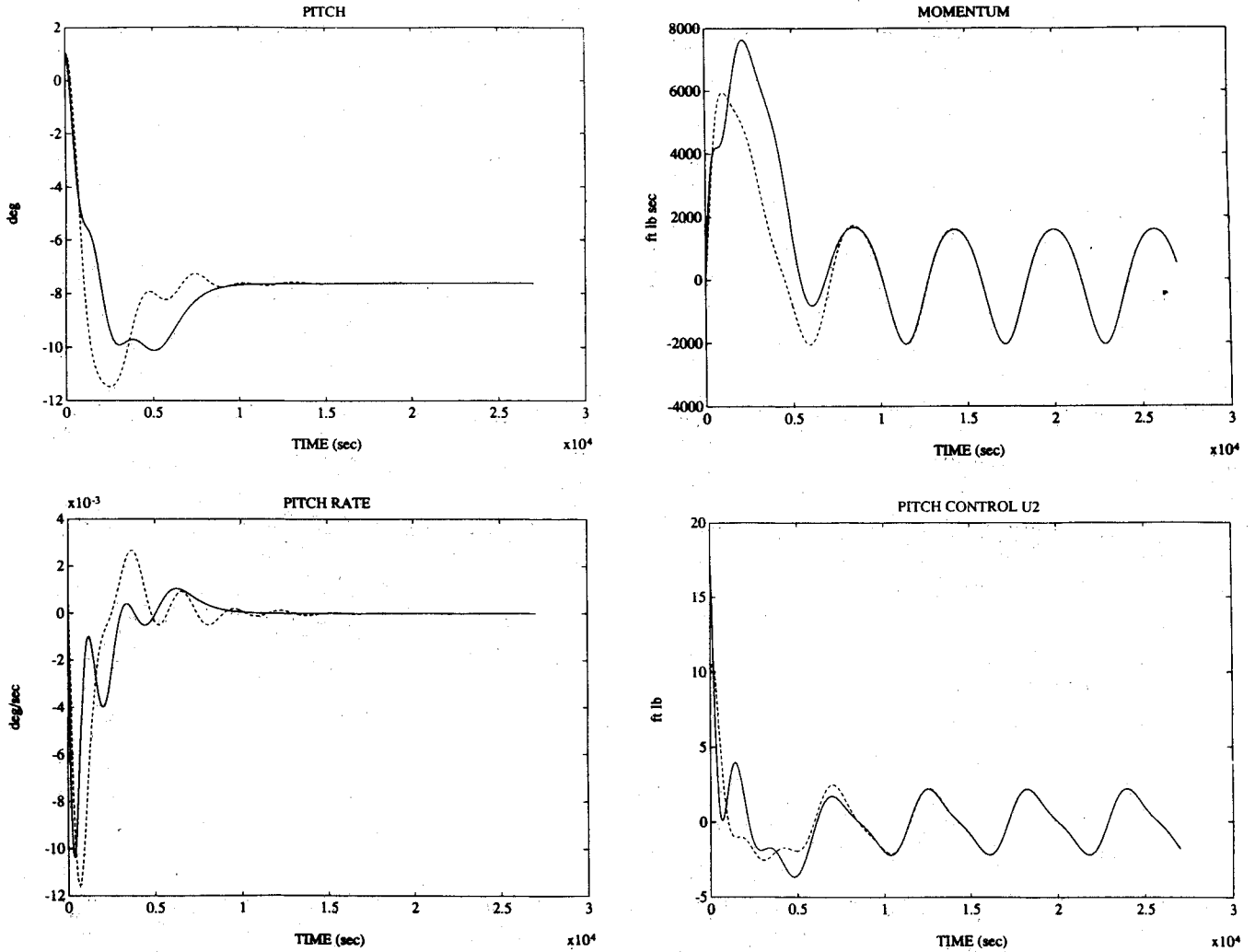


Fig. 4 Pitch axis response with disturbance rejection filter.

From the distribution of the eigenvalues, we observe that the eigenvalues of the controlled station in the pitch axis without the rejection filter (i.e., $-1.0n$, $-1.0n$, $-1.52n$, $-2.52n$) have been kept invariant for minimizing the control gains, while the eigenvalues of the uncontrolled rejection filter (i.e., $\pm 1.0nj$, $\pm 2.0nj$) have been optimally relocated from the imaginary axis (the line with a damping constant equal to zero) to the $-1.0n$ vertical line (the line with a damping constant equal to $1.0n$) on the negative real axis (i.e., $-1.0n \pm 1.0nj$, $-1.0n \pm 2.0nj$). One pair of the controlled rejection filter eigenvalues (i.e., $-1.0n \pm 1.0nj$) has a damping ratio exactly equal to 0.707, and the other pair (i.e., $-1.0n \pm 2.0nj$) has a damping ratio equal to 0.45, which lies outside the sector with a ± 45 -deg sector angle. By repeated application of the proposed procedure, we can place the pair in the desired sector. However, the procedure was not continued due to the observation that the pair in question has fairly good damping characteristics (i.e., the damping constant is $1.0n$ and the damping ratio is 0.45). The corresponding control gains are given as follows:

$$K_{PD} \triangleq [K_{A_2} \ K_{R_2} \ K_{H_2} \ K_{I_2} \ K_{\alpha_2} \ K_{\dot{\alpha}_2} \ K_{\beta_2} \ K_{\dot{\beta}_2}]$$

$$= [-6.4661E2 \ -3.3878E5 \ -2.0330E-2 \ -5.0184E-6 \ -2.9730E-4 \ -3.8668E-1 \ -6.2144E-4 \ -3.4480E-1]$$

(29)

The closed-loop response of the system is shown in Fig. 4. The asymptotic rejection of the aerodynamic disturbance is evidenced by the pitch attitude which becomes constant at

-7.5 -deg pitch TEA at about two orbits. Again, results from Ref. 6 using the LQR approach are included in Fig. 4.

Roll/Yaw Control Without Disturbance Rejection Filter

The roll/yaw controller for the system in Eq. (14) consists of two inputs, u_1 and u_3 , and eight states, including θ_1 , ω_1 , h_1 , \dot{h}_1 (roll axis) and θ_3 , ω_3 , h_3 , \dot{h}_3 (yaw axis). The control law is then given by

$$u_1 = -K_{A_1}\theta_1 - K_{R_1}\omega_1 - K_{H_1}h_1 - K_{I_1} \int h_1 - K_{A_3}\theta_3 - K_{R_3}\omega_3 - K_{H_3}h_3 - K_{I_3} \int h_3 \quad (30a)$$

$$u_3 = -\bar{K}_{A_1}\theta_1 - \bar{K}_{R_1}\omega_1 - \bar{K}_{H_1}h_1 - \bar{K}_{I_1} \int h_1 - \bar{K}_{A_3}\theta_3 - \bar{K}_{R_3}\omega_3 - \bar{K}_{H_3}h_3 - \bar{K}_{I_3} \int h_3 \quad (30b)$$

The uncontrolled station is unstable in roll/yaw with poles at $0, 0, \pm 1.0nj$, and $(\pm 1.05 \pm 0.7j)n$. As in the pitch axis case, we go to step 1 of the continuous design procedure.

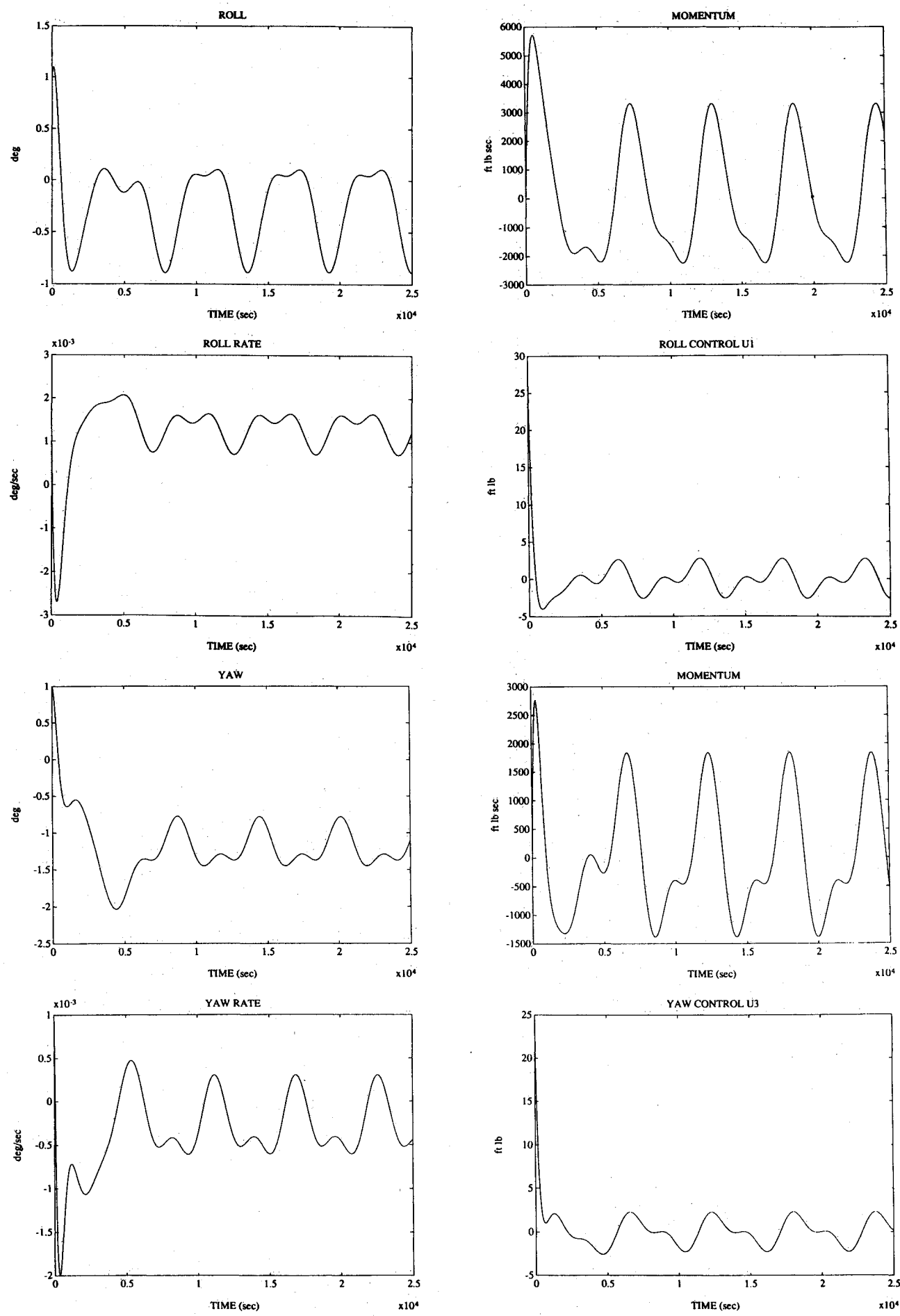


Fig. 5 Roll/yaw response without disturbance rejection filter.

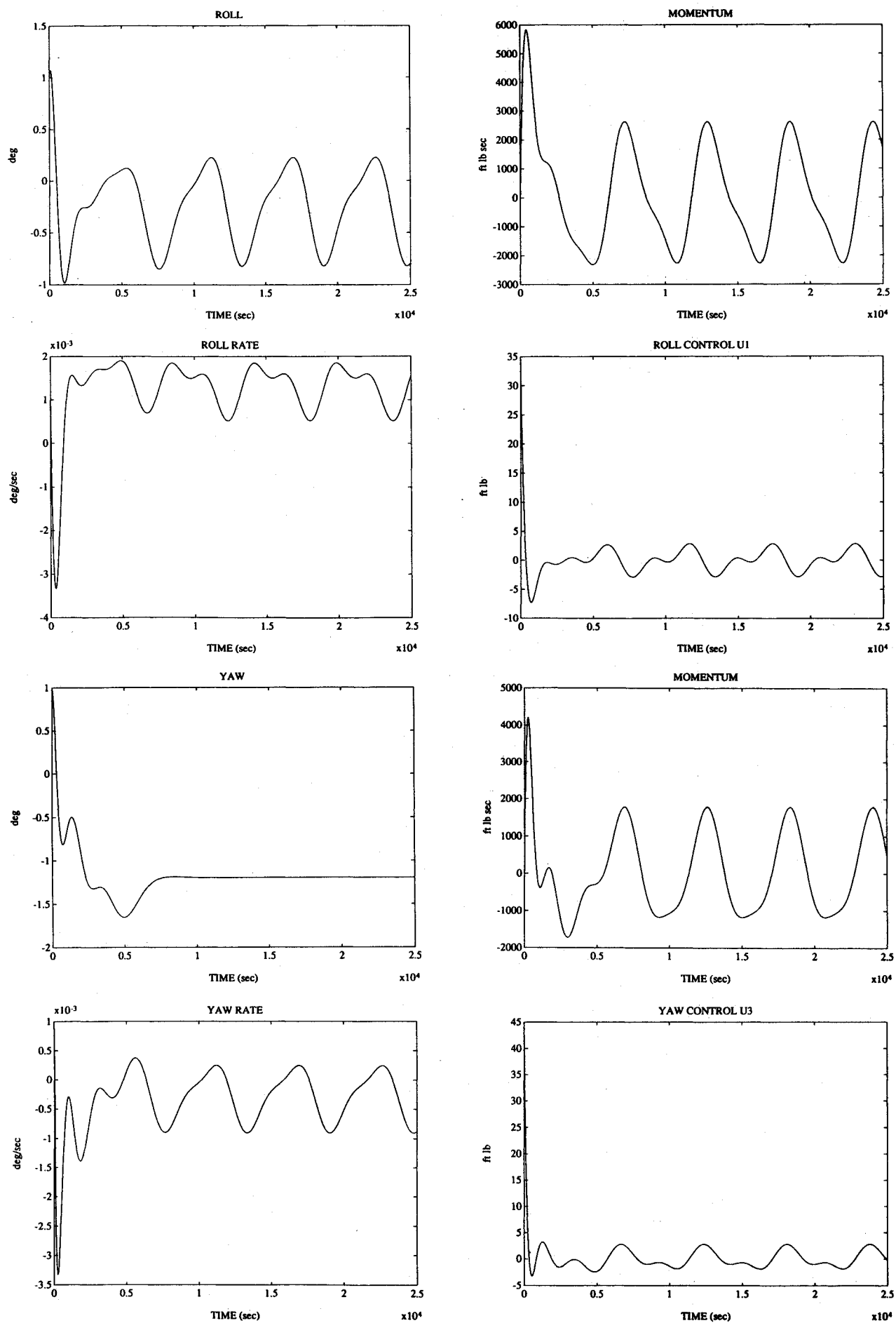


Fig. 6 Roll/yaw response with disturbance rejection filter.

Again, we set $\alpha = 0.5n$ and use the matrix sign function to solve the Riccati equation and obtain the matrix A_1 . The eigenvalues of A_1 are located at

$$\begin{aligned} &-1.0n, -1.0n, (-1.0 \pm 1.0j)n, \\ &(-1.05 \pm 0.7j)n, (-2.05 \pm 0.7j)n \end{aligned}$$

Thus, we see the eigenvalues of A_1 lie within the region of Fig. 2. The corresponding control gains are given as follows:

$$\begin{aligned} K_{RY} &\triangleq \begin{bmatrix} K_{A_1} & K_{R_1} & K_{H_1} & K_{I_1} & K_{A_3} & K_{R_3} & K_{H_3} & K_{I_3} \\ \bar{K}_{A_1} & \bar{K}_{R_1} & \bar{K}_{H_1} & \bar{K}_{I_1} & \bar{K}_{A_3} & \bar{K}_{R_3} & \bar{K}_{H_3} & \bar{K}_{I_3} \end{bmatrix} \\ &= \begin{bmatrix} -9.5746E2 & -6.1390E5 & -5.5096E-3 & 2.2936E-6 & -1.4405E2 & 2.0593E5 & 4.5858E-3 & 2.590E-6 \\ -3.2524E2 & -1.4063E5 & -1.7273E-3 & -2.6038E-6 & -4.0321E2 & -4.9358E5 & -3.9067E-3 & 8.094E-7 \end{bmatrix} \end{aligned} \quad (30c)$$

The closed-loop responses of the system to the aerodynamic disturbances of Table 1, with initial conditions of $\theta_1(0) = \theta_3(0) = 1$ deg and $\omega_1(0) = \omega_3(0) = 0.001$ deg/s, are shown in Fig. 5. Again we see periodic oscillations in both attitude and momentum due to aerodynamics.

Roll/Yaw Control with Disturbance Rejection Filter

As discussed in Ref. 6, cyclic disturbance filtering is possible for roll axis CMG momentum and yaw axis attitude but not the roll axis attitude. In this paper, a rejection filter for yaw attitude is considered.

The rejection filter equations for yaw attitude are given in Eq. (11b). The roll/yaw control logic for the system in Eq. (14) is given by

$$\begin{aligned} u_1 &= -K_{A_1}\theta_1 - K_{R_1}\omega_1 - K_{H_1}h_1 - K_{I_1} \int h_1 - K_{A_3}\theta_3 - K_{R_3}\omega_3 \\ &\quad - K_{H_3}h_3 - K_{I_3} \int h_3 - K_{\alpha_3}\alpha_3 - K_{\dot{\alpha}_3}\dot{\alpha}_3 - K_{\beta_3}\beta_3 - K_{\dot{\beta}_3}\dot{\beta}_3 \end{aligned} \quad (31a)$$

$$\begin{aligned} u_3 &= -\bar{K}_{A_1}\theta_1 - \bar{K}_{R_1}\omega_1 - \bar{K}_{H_1}h_1 - \bar{K}_{I_1} \int h_1 - \bar{K}_{A_3}\theta_3 - \bar{K}_{R_3}\omega_3 \\ &\quad - \bar{K}_{H_3}h_3 - \bar{K}_{I_3} \int h_3 - \bar{K}_{\alpha_3}\alpha_3 - \bar{K}_{\dot{\alpha}_3}\dot{\alpha}_3 - \bar{K}_{\beta_3}\beta_3 - \bar{K}_{\dot{\beta}_3}\dot{\beta}_3 \end{aligned} \quad (31b)$$

Proceeding as before, the closed-loop eigenvalues are located at

$$\begin{aligned} &-1.0n, -1.0n, (-1.0 \pm 1.0j)n, (-1.0 \pm 1.0j)n \\ &(-1.05 \pm 0.7j)n, (-2.05 \pm 0.7j)n, (-1.0 \pm 2.0j)n \end{aligned}$$

Similar to the pitch control case, the eigenvalues of the controlled station in roll/yaw without the rejection filter are kept invariant to minimize the control gains, whereas one pair of the eigenvalues of the controlled rejection filter (i.e., $-1.0n \pm 2.0nj$) is retained outside the desired sector due to fairly good damping characteristics. The corresponding control gains are given as follows:

$$\begin{aligned} K_{RYD} &\triangleq \begin{bmatrix} K_{A_1} & K_{R_1} & K_{H_1} & K_{I_1} & K_{A_3} & K_{R_3} & K_{H_3} & K_{I_3} & K_{\alpha_3} & K_{\dot{\alpha}_3} & K_{\beta_3} & K_{\dot{\beta}_3} \\ \bar{K}_{A_1} & \bar{K}_{R_1} & \bar{K}_{H_1} & \bar{K}_{I_1} & \bar{K}_{A_3} & \bar{K}_{R_3} & \bar{K}_{H_3} & \bar{K}_{I_3} & \bar{K}_{\alpha_3} & \bar{K}_{\dot{\alpha}_3} & \bar{K}_{\beta_3} & \bar{K}_{\dot{\beta}_3} \end{bmatrix} \\ &= \begin{bmatrix} -1.3348E3 & -8.5335E5 & -8.8180E-3 & 3.7827E-6 & 6.1431E1 & 3.0567E5 & 5.4920E-3 & \\ -3.8116E2 & -3.3496E5 & -6.3889E-3 & -4.4046E-6 & -1.3072E3 & -4.5138E5 & -2.4012E-4 & \\ 2.7027E-6 & 1.7653E-4 & 4.2740E-2 & -1.2852E-3 & 2.9721E-1 & & & \\ 2.5368E-6 & 5.0171E-4 & -7.6719E-1 & 2.1461E-4 & -7.7796E-1 & & & \end{bmatrix} \end{aligned} \quad (31c)$$

The responses to the same disturbances and initial conditions given in the roll/yaw control without disturbance rejection filter are shown in Fig. 6. The yaw attitude approaches a steady-state value, and the yaw axis CMG momentum continues to oscillate but at a lower peak-to-peak magnitude. The roll attitude is unchanged.

Conclusions

This paper presents a multivariable design approach using optimal regional pole assignment. A new sequential procedure

is used for optimally placing the closed-loop poles of a continuous time system within the common region of an open sector with a sector angle ± 45 deg from the negative real axis and the left-hand side of a line parallel to the imaginary axis in the complex s plane without explicitly using the eigenvalues of the open-loop system. The proposed optimal regional pole assignment method provides an efficient procedure to select the state weighting matrix for the linear quadratic optimal design of a space station. The sensitivity of the design to modeling errors and the extension of the proposed optimal regional pole assignment method to include a closed sector with a sector angle less than 45 deg are under study.

Appendix

Matrix Sign Function²

The matrix sign function of a matrix $A \in \mathbb{C}^{n \times n-1-3}$ is defined as

$$\text{sign}(A) = A(\sqrt{A^2})^{-1} = A^{-1}(\sqrt{A^2}) \quad (A1)$$

where the matrix $\sqrt{A^2}$ denotes the principal square root of A^2 . A fast and stable algorithm³ to compute the matrix sign function is listed below. For $k = 0, 1, \dots$,

$$\begin{aligned} P_j(k) &= P_{j-1}(k) + S^{-2}(k)Q_{j-1}(k), \quad P_1(k) = Id_n \\ Q_j(k) &= P_{j-1}(k) + Q_{j-1}(k), \quad Q_1(k) = Id_n, \quad \text{with } j = 2, \dots, r \end{aligned} \quad (A2a)$$

$$S(k+1) = S(k)Q_r^{-1}(k)P_r(k), \quad S(0) = A, \quad \lim_{k \rightarrow \infty} S(k) = \text{sign}(A) \quad (A2b)$$

where r is the order of the desired rate of convergence.

Solving the Riccati Equation via the Matrix Sign Function

The Riccati equation for the controllable continuous time system (A, B) with weighting matrices $Q (\geq 0)$ and $R (> 0)$ is given by

$$PBR^{-1}B^TP - A^TP - PA - Q = 0n \quad (A3a)$$

The steady-state solution of this Riccati equation, $P (\geq 0)$ with (Q, A) detectable, can be easily computed using the properties of the matrix sign function.^{13,14} Consider the Hamiltonian associated with the given system

$$H = \begin{bmatrix} A & -BR^{-1}B^T \\ -Q & -A^T \end{bmatrix} \quad (\text{A3b})$$

The following algorithm can be used to obtain the solution P :

$$H_{k+1} = (1/2)[H_k + H_k^{-1}], \quad H_0 = H, \quad \text{and} \quad \lim_{k \rightarrow \infty} H_k = \text{sign}(H) \quad (\text{A4a})$$

Let

$$\text{sign}^+(H) \triangleq (1/2)[Id_{2n} + \text{sign}(H)] \triangleq \begin{bmatrix} X_{11} & X_{12} \\ X_{21} & X_{22} \end{bmatrix} \quad (\text{A4b})$$

Then, we have

$$P = -(X_{22})^{-1}X_{21} = -(X_{12})^{-1}X_{11} \quad (\text{A5})$$

To alleviate the problems of computing H_k^{-1} , the Hamiltonian can be transformed into a symmetric form as follows¹⁴:

$$\hat{H} = \hat{J}H = \begin{bmatrix} 0_n & -Id_n \\ Id_n & 0_n \end{bmatrix} H = \begin{bmatrix} Q & A^T \\ A & -BR^{-1}B^T \end{bmatrix} \quad (\text{A6a})$$

Then, the algorithm Eq. (A4) becomes

$$\hat{H}_{k+1} = (1/2)[\hat{H}_k + \hat{J}\hat{H}_k^{-1}\hat{J}], \quad \hat{H}_0 = \hat{J}H$$

$$\lim_{k \rightarrow \infty} (-\hat{J}\hat{H}_k) = \text{sign}(H) \quad (\text{A6b})$$

The computation of the inverse of the symmetric matrix \hat{H}_k is much simpler than computing the inverse of H_k . The Riccati solution P is again given by Eq. (A5).

Acknowledgments

This work was supported in part by the U.S. Army Research Office, under contract DAAL-03-87-K0001, and NASA-Johnson Space Center, under Grants NAG 9-380 and NAG 9-385.

The authors wish to express their gratitude for the valuable remarks and suggestions made by the reviewers.

References

- ¹Shieh, L. S., and Tsay, Y. T., "Algebra-Geometric Approach for the Model Reduction of Large-Scale Multivariable Systems," *IEEE Proceedings*, Vol. 131, Pt. D, No. 1, 1984, pp. 23-36.
- ²Shieh, L. S., Tsay, Y. T., and Yates, R. E., "Some Properties of Matrix Sign Functions Derived From Continued Fractions," *IEEE Proceedings*, Vol. 130, Pt. D, No. 3, 1983, pp. 111-118.
- ³Shieh, L. S., Lian, S. R., and McInnis, B. C., "Fast and Stable Algorithms for Computing the Principal Square Root of a Complex Matrix," *IEEE Transactions on Automatic Control*, Vol. AC-32, No. 9, 1987, pp. 820-822.
- ⁴Wie, B., and Bryson, A. E., "On Multivariable Control Robustness Examples: A Classical Approach," *Journal of Guidance, Control, and Dynamics*, Vol. 10, No. 1, 1987, pp. 118-120.
- ⁵Bryson, A. E., "Control of Spacecraft and Aircraft," Class Notes, Stanford Univ., Stanford, CA, 1987.
- ⁶Wie, B., Byun, K., Warren, V., Geller, D., Long, D., and Sunkel, J., "A New Momentum Management Controller for the Space Station," AIAA Paper 88-4132, Aug. 1988.
- ⁷Anderson, B. D. O., and Moore, J. B., *Linear Optimal Control*, Prentice-Hall, Englewood Cliffs, NJ, 1971.
- ⁸Ackermann, J., *Sampled-Data Control Systems*, Springer-Verlag, New York, 1985, p. 234.
- ⁹Shieh, L. S., Dib, H. M., and McInnis, B. C., "Linear Quadratic Regulators with Eigenvalue Placement in a Vertical Strip," *IEEE Transactions on Automatic Control*, Vol. AC-31, No. 3, 1986, pp. 241-243.
- ¹⁰Shieh, L. S., Dib, H. M., and Ganesan, S., "Linear Quadratic Regulators with Eigenvalue Placement in a Horizontal Strip," *International Journal of System Science*, Vol. 19, No. 7, 1987, pp. 1279-1290.
- ¹¹Kawasaki, N., and Shimemura, E., "Determination of Quadratic Weighting Matrices to Locate Poles in a Specified Region," *Automatica*, Vol. 19, No. 5, 1983, pp. 557-560.
- ¹²Shieh, L. S., Dib, H. M., and Ganesan, S., "Continuous-Time Quadratic Regulators and Pseudo-Continuous-Time Quadratic Regulators with Pole Placement in a Specific Region," *IEEE Proceedings*, Vol. 134, Pt. D, No. 5, 1987, pp. 338-346.
- ¹³Shieh, L. S., Tsay, Y. T., Lin, S. W., and Coleman, N. P., "Block-Diagonalization and Block-Triangularization of a Matrix Via the Matrix Sign Function," *International Journal of Systems Science*, Vol. 15, No. 11, 1984, pp. 1203-1220.
- ¹⁴Bierman, G. J., "Computational Aspects of the Matrix Sign Function Solution to the ARE," *Proceedings of the 23rd Conference Decision on Control*, 1984, pp. 514-519.